Title	Toward the development of a fundamentally based chemical model for cyclopentanone: high-pressure-limit rate constants for H atom abstraction and fuel radical decomposition
Author(s)	Zhou, Chong-Wen; Simmie, John M.; Pitz, William J.; Curran, Henry J.
Publication Date	2016-08-25
Publication Information	Zhou, Chong-Wen, Simmie, John M., Pitz, William J., & Curran, Henry J. (2016). Toward the Development of a Fundamentally Based Chemical Model for Cyclopentanone: High-Pressure-Limit Rate Constants for H Atom Abstraction and Fuel Radical Decomposition. The Journal of Physical Chemistry A, 120(36), 7037-7044. doi: 10.1021/acs.jpca.6b03994
Publisher	American Chemical Society
Link to publisher's version	http://dx.doi.org/10.1021/acs.jpca.6b03994
Item record	http://hdl.handle.net/10379/6865
DOI	http://dx.doi.org/10.1021/acs.jpca.6b03994

Towards the Development of a Fundamentally-based Chemical Model for Cyclopentanone: High Pressure Limit Rate Constants for H-atom Abstraction and Fuel Radical Decomposition

Chong-Wen Zhou,*,† John M. Simmie,† William J. Pitz,‡ and Henry J. Curran†

†*School of Chemistry & Combustion Chemistry Centre, National University of Ireland Galway, H91 TK33 Ireland*

‡*Lawrence Livermore National Laboratory, Livermore, California 94550, United States*

E-mail: chongwen.zhou@nuigalway.ie

Abstract

Theoretical aspects of the development of a chemical kinetic model for the pyrolysis and combustion of a cyclic ketone, cyclopentanone, are considered. Calculated thermodynamic and kinetic data are presented for the first time for the principal species including 2- and 3-oxo-cyclopentyl radicals which are in reasonable agreement with the literature. These radicals can be formed via H-atom abstraction reactions by $\dot{\mathrm{H}}$ and $\ddot{\mathrm{O}}$ atoms, and $\dot{\mathrm{O}}\mathrm{H}$, $\mathrm{H}\dot{\mathrm{O}}_2$, and $\dot{\mathrm{C}}\mathrm{H}_3$ radicals, the rate constants of which have been calculated. Abstraction from the β hydrogen atom is the dominant process when $\dot{\mathrm{O}}\mathrm{H}$ is involved but the reverse holds true for $\mathrm{H}\dot{\mathrm{O}}_2$ radicals. The subsequent β-scission of the radicals formed are also determined and it is shown that recent tunable VUV photoionization mass spectrometry experiments can be interpreted in this light. The bulk

of the calculations used the composite model chemistry G4 which was benchmarked in the simplest case with a coupled cluster treatment, CCSD(T), in the complete basis set limit.

Introduction

Bio-derived fuels can be used to displace fossil fuels in practical combustion devices to lower greenhouse-gas emissions. Cyclopentanone is a ketone that can be bio-derived because this chemical class is formed when fungi break down cellulose, a major component of biomass.[1,2] Moreover, cyclopentanone is a component in mixtures formed from the pyrolysis of biomass, for example, during the fast pyrolysis of aspen wood chips.[3]

Cyclopentanone has fuel properties that are attractive for applications in spark-ignition internal-combustion engines. It has the lowest autoignition reactivity of a number of biofuels.[4] These properties make cyclopentanone especially attractive as a blending component for use in boosted spark-ignition engines because of its resistance to autoignition. Downsized, boosted spark-ignition engines are an attractive technology that allows higher efficiencies than most current spark-ignition engines in the light-duty ground transportation market.[5] This means cyclopentanone is not only attractive because it can be bio-derived, but also because its properties allow gains in engine efficiency; both of these characteristics yield potential reductions in greenhouse gas emissions. Cyclopentanone forms dimers[6] through quite weak hydrogen bond interactions C$-$H$\cdots$O which probably accounts for its higher density and boiling point in comparison to the acyclic diethyl ketone.

Engine simulations can be used to assess the potential of cyclopentanone as a blending agent in gasoline, but these require a chemical kinetic model to simulate its ignition properties; such a mechanism is not currently available. The mechanism needs to be valid for use in predicting combustion in both spark ignition and compression ignition engines. This means the mechanism should be predictive for end-gas autoignition and flame speed, and ignition phasing in a homogeneous-ignition compression-ignition engine. To achieve this predictivity,

it is recommended that the mechanism should to be valid for conditions of pressure from 3 to 50 atm, at temperatures from 600 K to 1500 K, at a dilution of up to 20% (by exhaust gas recirculation) and at equivalence ratios of 0.5 to 1.0. The objective of this work is to provide rate constants and product channels needed to support the development of a chemical kinetic mechanism for cyclopentanone.

The molecular reactions of a six-membered cyclic ketone, cyclohexanone, has been studied by Zaras et al.[7] at the G3B3 level of theory. In a companion experimental work on cyclohexanone oxidation in a jet-stirred reactor they discuss qualitatively the fate of the three radicals produced by H-atom abstraction from the parent ketone.[8]

To achieve predictability, accurate rate constants are needed. At low and intermediate temperatures where autoignition reactions occur, chemical kinetic mechanisms for fuels are particularly sensitive to H-atom abstraction rates by $\dot{O}H$ and $H\dot{O}_2$ radicals. Providing accurate rate constants for these reactions will contribute to the prediction of engine knock. For flame speed predictions, accurate rate constant of hydrogen atom abstraction by hydrogen atoms may also be helpful. Additionally, the decomposition rate constants for fuel radicals formed from these hydrogen-atom abstraction reactions are also needed in high temperature fuel reactivity predictions. The decomposition of a cyclopentanone radical is more complicated than that of the much-studied acyclic alkyl radical, and involves the opening of a ring containing a ketone group. It is difficult to estimate its rate constant by analogy to other radical decompositions whose rate constants are available in the literature.

Zaras et al.[9] have calculated barrier heights for the decomposition of cyclopentanone at the G3B3 level of theory and also calculate accompanying rate constants. Low temperature oxidation pathways of cyclic ketones have been explored by Scheer et al.[10] who focused primarily on the subsequent reactions of the initial radicals with oxygen. Furthermore, Xia and colleagues[11] have reported on the excited-state ring-opening mechanisms of cyclic ketones including cyclopentanone without further investigation of the ring-opening rate constants.

In this paper, rate constants for H-atom abstraction from cyclopentanone by $\dot{O}H$, $H\dot{O}_2$

and $\dot{C}H_3$ radicals and $\dot{H}$ and $\ddot{O}$ atoms are calculated using ab initio methods. In addition the rate constants for cyclopentanone radical decompositions are also computed. These key rate constants and their associated product channels will help towards the development of a detailed chemical kinetic mechanism to describe cyclopentanone oxidation.

Computational methodology

Optimized geometries, frequencies, international rotational potentials, and energies of the stable complexes and saddle points along the intrinsic reaction coordinate (IRC) were calculated at the M062X/6-311++G(d,p) level of theory.[12] Geometry optimization was followed by vibrational frequency analysis to verify the local minima (number of imaginary frequencies equal to zero) or first order saddle points (number of imaginary frequencies equal to one) character of the compounds. Intrinsic reaction coordinate (IRC) calculations[13,14] are carried out to calculate the connection between transition states and the reactant or product complexes.

To achieve more reliable energies of the various species along the potential energy surfaces, we have employed the CCSD(T) (coupled-cluster approach with single and double substitutions including a perturbative estimate of connected triples substitutions) method with the correlation-consistent polarized split-valence multiple-ζ basis sets, cc-pVTZ, and cc-pVQZ[15] for hydrogen abstraction by $\dot{O}H$ radicals. The CCSD(T) total energies were extrapolated to the complete basis set (CBS) limit according to the procedure of Halkier *et al.*:[16]

$$E_{\mathrm{CBS}} = [E_X X^3 - E_{X-1}(X-1)^3]/[X^3 - (X-1)^3]$$

where $X = 4$ for the cc-pVQZ basis set. All the single point energy calculations mentioned above are based on the M062X/6-311++G(d,p) geometries. The T_1 diagnostics for pre- and post- reaction complexes and transition states are all lower than the critical 0.02 value, and so that single-reference methods are expected to give an adequate description of the wave

function.[17] Single point energy calculations using the CCSD(T) method were carried out using the Molpro program.[18] The CCSD(T)/CBS methodology is computationally expensive and sometimes failed to converge, so only certain key processes were undertaken at this level of theory in order to benchmark the G4 method which was used for all of the electronic energy calculations in this work.[19] Electronic structure calculations were performed using the Gaussian-09[20] application.

The zero-point corrected electronic energies barrier heights using the G4 method were used in conjunction with scaled frequencies and rotational constants to calculate the high-pressure limit rate constants in the temperature range of 500–2000 K. The low-frequency torsional modes were treated as hindered rotors using a Pitzer-Gwinn-like approximation except for those transition states involving abstraction by a methyl radical where a free rotor approximation was used due to the very low rotational barrier. The hindrance potentials were determined for every geometry around all possible dihedral angles by fitting Fourier series to the M062X/6-311++G(d,p) energies along the relaxed internal rotation. The remaining conserved modes were treated as harmonic oscillators. Eckart asymmetric tunneling corrections were included.[21] Variflex and Multiwell were used to carry out these rate coefficient calculations.[22–24] The thermochemical calculations were performed using the Thermo module of Multiwell.

RESULTS AND DISCUSSION

Geometry of cyclopentanone

Cyclopentanone (CPO) is a non-planar five membered ring with C2 symmetry and the labelled structure is shown in Fig. 1; Cartesian coordinates, vibrational frequencies and rotational constants for CPO and other species are provided in the Supplemental Material. The hydrogen atoms occupy positions which may be loosely described as 'equatorial' (eq) and 'axial' (ax) at both the α-carbons adjacent to the ketonic group, C2 and C5, and the

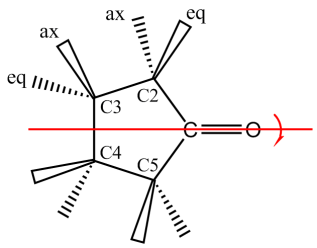

Figure 1: Cyclopentanone

β-carbons, C3 and C4, which are more remote.

The C–H bond dissociation energies at 298.15 K are C_α—H = 379 and C_β—H = 407 kJ mol^{-1} in satisfactory agreement with the corresponding values of 382 and 411 kJ mol^{-1} computed by Zaras et al.[9] (except that these refer to 0 K) and the CBS-QB3 values[10] of 378 and 407 kJ mol^{-1}. These values are to be compared to that for cyclopentane[25] where C—H = 400 ± 4 kJ mol^{-1}.

The enthalpy of formation at 298.15 K of -194.8 ± 6.4 kJ mol^{-1}, calculated by an atomization procedure,[26] is in good agreement with the most recent experimental determination[27] by reductive calorimetry of -197.4 ± 1.3 kJ mol^{-1} and with much earlier static bomb combustion calorimetric measurements of -194.8 ± 1.7 and -193.0 ± 1.8 kJ mol^{-1} by Wolf[28] and Sellers and Sunner.[29] The computed constant pressure heat capacity of gaseous CPO of 96.4 J K^{-1} mol^{-1} is in good agreement with the literature value[30] of 95.33 J K^{-1} mol^{-1}.

The $\Delta_f H°$(298.15 K) of 2-oxo-cyclopentyl (CPO-2) and 3-oxo-cyclopentyl (CPO-3) radicals have been calculated and they are -28.8 and -0.4 kJ mol^{-1}, respectively, with CPO-2 being considerably more stable because of the resonance stabilization of the CH⋯C⋯O moiety.

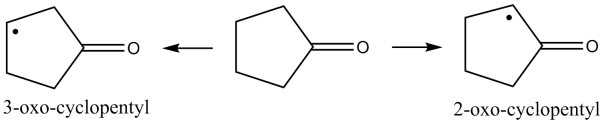

Figure 2: Cyclopentanone and its radicals

H-atom abstraction by $\dot{\text{O}}$H radical

Hydrogen atom abstraction reactions lead to the formation of the two oxo-cyclopentyl radicals as shown in Fig. 2. There are only four different abstractable H-atoms which can be described as 'equatorial' and 'axial' attached to α- and β-carbons. Table 1 lists the G4 zero-point corrected electronic energies of the pre- and post-reaction complexes, the transition states and the final products, all relative to the reactants. For the reaction channels involving the formation of van der Waals pre-reaction complexes, the rate constant for that reaction channel is determined by two reaction steps which are the formation of a weakly bound van der Waals complex and a H-atom abstraction step with a tight transition state.

Georgievskii and Klippenstein[31] have proposed a two transition state model to study the kinetics of the $C_2H_6 + \dot{C}N$ reaction and stated that, for those two step transition state reaction processes, the outer transition state forming the van der Waals complex is important and should be taken into consideration using variational transition state theory for temperatures lower than 300 K. However, for temperatures higher than 300 K, a single inner transition state description can be used for computing the rate constant. In *this work* the temperature range of interest is 500–2000 K so the kinetics of the formation of pre-reaction complexes has been neglected.

Electronic energies for the barriers of α eq, α ax, and β ax have also been calculated at the CCSD(T)/CBS level of theory, and the comparison with G4 results is shown in Table 1; the difference between those two methods ranges from 5.6 to 1.2 kJ mol^{-1} which is still within the uncertainty of the electronic energy calculations. The CCSD(T)/CBS energies are not shown for the β eq site because the electronic energy calculation for the transition state did not converge.

Typically H-atom abstraction from oxygenates by $\dot{\text{O}}$H radicals involves the formation of weakly-bound pre- and post-reaction complexes and this system is no exception; Fig. 3 shows a schematic of abstraction from the 'equatorial' hydrogen at an α-carbon. The zero point energies of the pre- and post-reaction energies are shown in Table 1, while no pre- or

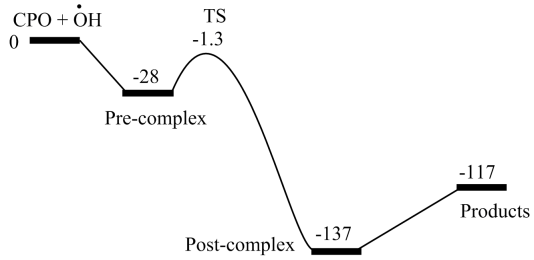

Figure 3: Potential energy surface for channel α eq, kJ mol^{-1} at G4 level of theory (0 K).

post- reactions complexes were found for the β eq site. The stabilisation of the pre-reaction complex, relative to the reactants, amounts to 28 kJ mol^{-1} and that of the post-reaction complex, relative to the final products, is 20 kJ mol^{-1}. This is typical of values encountered in many similar systems as recorded by Galano and colleagues.[32]

Tunneling, evaluated with the Eckart model, plays a role in these reactions and cannot be ignored for temperatures lower than 1000 K. Taking the reaction channel α eq as an example, the rate constant ratio with/without tunneling is 1.8 at 500 K and decreases to 1.2 at 1000 K.

Table 1: Zero-point corrected electronic energies at G4 and (CCSD(T)/CBS) / kJ mol^{-1}

Site	Pre-	TS	Post-	Prod.
		H-abstraction by ȮH radical		
α eq	−28.1	−1.26 (4.32)	−137.3	−116.7 (−111.7)
α ax	−28.1	4.10 (1.21)	−137.3	−116.7 (−111.7)
β eq	—	4.10	—	−89.6 (−86.0)
β ax	−28.1	0.62 (−0.15)	−98.0	−89.6 (−86.0)
		H-abstraction by HȮ$_2$ radical		
α eq	−47.5	63.3	−13.0	14.8
α ax	−47.6	57.3	−13.1	14.8
β eq	−14.5	69.4	30.3	41.9
β ax	−47.5	60.9	22.0	41.9

The high-pressure rate constants were obtained using the barrier heights computed by the G4 method because these computations were tractable for all the reactions considered in this work. For H-atom abstraction by ȮH radicals from the adjacent or α-carbon atoms C2 and C5 to yield the CPO-2 radical the total rate constant is calculated to be, in cm^3 mol^{-1}

s^{-1}:

$$k_\alpha = 2.34 \times 10^3 T^{3.04} \exp(817/T)$$

and that from the remote β-carbon atoms C3 and C4 to give CPO-3:

$$k_\beta = 1.13 \times 10^5 T^{2.58} \exp(626/T)$$

Thus, over the fitting range of 500–2000 K abstraction predominantly occurs from the β positions decreasing slightly as the temperature increases, Fig. 4a.

There is no data in the literature against which these calculations can be tested except for a single room temperature measurement by Dagaut et al.,[33] using a flash photolysis resonance fluorescence technique, who reported $k = (1.77 \pm 0.11) \times 10^{12}$ cm^3 mol^{-1} s^{-1} with the corresponding value obtained *here* of $k_\alpha + k_\beta = 3.51 \times 10^{12}$ cm^3 mol^{-1} s^{-1} with this prediction being a factor of two faster than that measured by Dagaut et al.[33]

Abstraction from the β carbon atoms is always faster than from the α carbon atoms, Fig. 4a. Even though the reaction barrier is 1.9 kJ mol^{-1} lower for the α eq position; the α ax and β eq hydrogen atoms have the same barriers and the rate constant are almost identical in the entire temperature range.

Rate constants for the β axial channel are about a factor of 2.5 higher than the α equatorial channel, Fig. 4b. A comparison of the relaxed potential energy scans for the C····H····O—H internal rotor for the two relevant transition states shows a significant difference, Fig. 5. The reaction channel forming an α equatorial radical is about 16 kJ mol^{-1} which is typical of a hindered rotor but for the β axial reaction channel it is only 2.5 kJ mol^{-1} — effectively a free rotor. The root cause of the difference is the interaction that occurs as the hydrogen atom in the OH group moves closer to the ketonic oxygen, forming in essence a six-membered ring system.

In summary, the hydrogen bond formed in the transition state leads to a relatively stable six-membered-ring structure and thereby lowers the barrier height but also lowers the entropy

of that reaction channel. The final rate constants are determined by the competition between these two parameters, and in this case the entropy terms dominates and k_α equatorial is smaller than k_β axial.

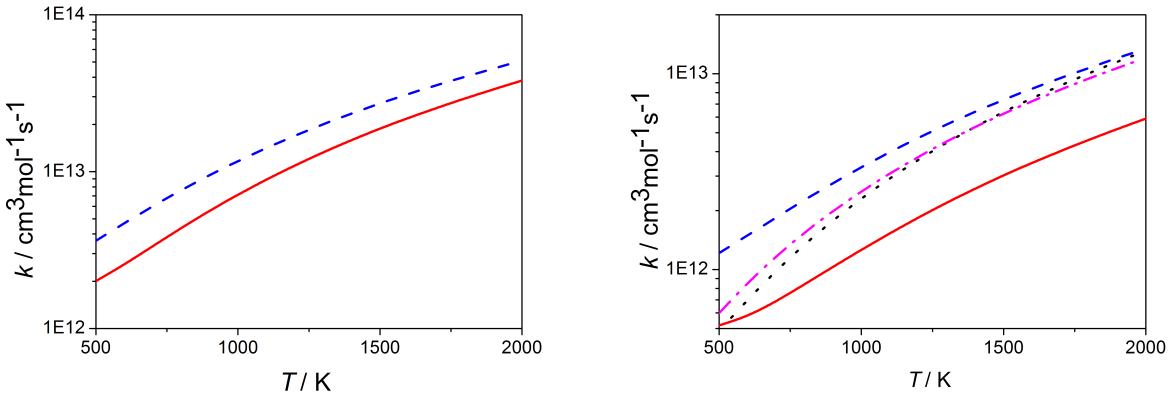

Figure 4: (a) Total rate constants for H-abstraction by $\dot{O}H$ radical from CPO to form CPO-2 (—) and CPO-3 (– – –). (b) Single channel rate constant (per H-atom) for hydrogen abstraction by $\dot{O}H$ radical from CPO. α eq —, β ax – – –, α ax $\cdots$, β eq, – · –.

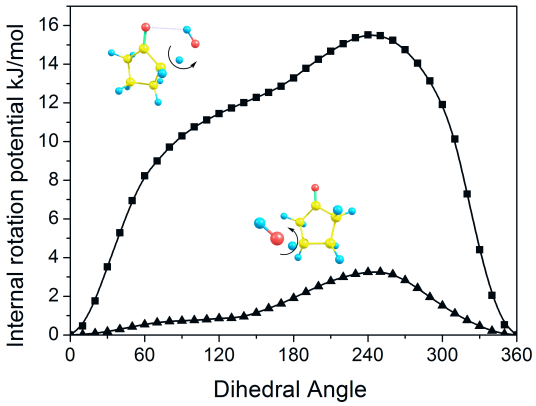

Figure 5: C····H····O—H internal rotor in transition states: ■ α eq, ▲ β ax.

Chemical kinetic rate constants depend upon both geometry and frequency calculations since these determine the rotational and vibrational partition functions. Two sets of frequency modes and rotational constants have been calculated at the B3LYP/6-311(2df,p) (the geometry optimizer in G4 theory) and M062X/6-311++G(d,p) levels of theory for both

reactants and transition state for the α eq channel. However the difference between the final rate constants from these two approaches is negligible, with a maximum difference of only 3.5%, Fig. S3. Thus, the uncertainty in the rate constants arising from different approaches to determine the partition functions can be neglected.

H-atom abstraction by $H\dot{O}_2$ radical

As observed for the $\dot{O}H$ radical, the hydroperoxyl radical forms both pre- and post-reaction complexes which are typically more stabilized, Fig. 6. However, there are differences: the hydroperoxyl radical abstraction reaction has higher barriers which lie above the entrance channel and has endothermic rather than exothermic products. Relative electronic energies for pre-reaction complexes, transition states and post-reaction complexes are also shown in Table 1. All of the electronic energies for the H-atom abstraction by $H\dot{O}_2$ radicals are reported at the G4 level of theory in this work.

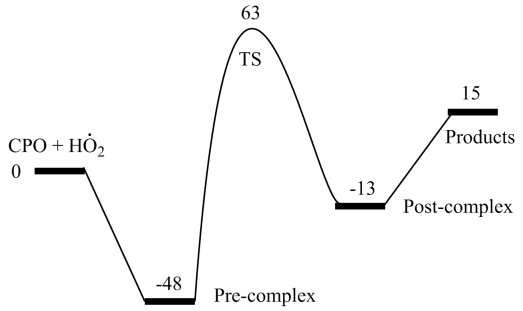

Figure 6: Potential energy surface for channel α eq, kJ mol^{-1} at G4 level of theory (0 K).

A comparison of the internal rotation of the HO_2 fragment in the transition states of α equatorial and β equatorial is shown in Fig. 7. As previously, there is a difference because of the interaction of OOH with the ketonic oxygen although this time a seven-membered ring is formed. However, the difference is not as pronounced as was the case for $\dot{O}H$ abstraction and this is reflected in the computed rate constants.

Total rate constants for abstraction by $H\dot{O}_2$ radicals are calculated to be (in units of cm^3

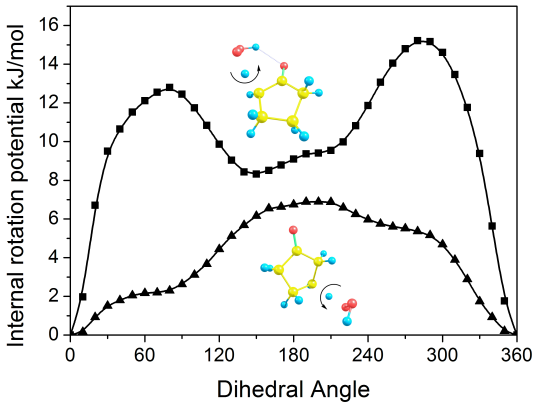

Figure 7: H···O—O—H hindered rotor in transition states: ■ α eq, and ▲ β eq.

mol^{-1} s^{-1}):

$$k_\alpha = 9.91 \times 10^{-4} T^{4.74} \exp(-5,040/T)$$
$$k_\beta = 5.45 \times 10^{-2} T^{4.27} \exp(-5,957/T)$$

For abstraction by $\dot{H}O_2$ radicals twice as much 2-oxo-cyclopentyl radical is formed at 500 K in comparison to the 3-oxo radical; this ratio diminishes with increasing temperature until it approaches unity at 1800 K.

H-atom abstraction by $\dot{H}$ and $\ddot{O}$ atoms and $\dot{C}H_3$ radicals

Barriers and reaction energies as well as site-specific rate constants (sum of the rate constants for abstracting the same type of hydrogen atom) in a modified Arrhenius format are shown in Table 2 for H-atom abstraction from CPO by $\dot{H}$ and $\ddot{O}$ atoms and $\dot{C}H_3$ radicals. The values obtained for abstraction by $\dot{H}$ atoms are comparable to those for tetrahydrofuran (THF) although these were computed at a different level of theory.[34] The α-carbon positions are somewhat more reactive than the β-carbons but the differences are slight.

For H-atom abstraction by $\dot{C}H_3$ radicals, the rate constant for the α channel is faster than that for the β channel over the entire temperature range investigated here (500 – 2000 K),

Fig. 8a. Rate constants for both channels are faster than for abstraction of the secondary hydrogen atom in an n-alkane provided by Manion et al.[35] The electronic energy barrier heights for abstraction of the β hydrogen atom are 6.8 kJ mol^{-1} (β eq) and 11.5 kJ mol^{-1} (β ax) *lower* than abstraction of the β H-atom in THF and the rate constant from the CPO-3 (β) site is faster than for the β site in THF.

For H-atom abstraction by $\dot{\text{H}}$ atoms, the α rate constant is faster than the β rate constant at temperatures below 2000 K, Fig. 8b. The α rate constant is close to the rate for H-atom abstraction in cyclopentane.[36] The rate constant of hydrogen atom abstraction from the CPO-3 (β) site is about 10 times lower at 900 K than the analogous C3 or β-carbon site in THF.

It is interesting to note that in the case of H-atom abstraction by $\ddot{\text{O}}$ atoms, Fig. 8c, the rate constants of the α pathway are lower than that for the β pathway even though the C–H bond strength at the α site is much weaker. The α-transition states are 'early' whilst the β-transition states are 'late' viewed from the perspective of the C$\cdots$H and the H$\cdots$O bond distances, viz. α 1.23 and 1.31 versus β 1.27 and 1.25 Å. The abstraction rate constant from the β site of CPO is within a factor of two of reported rate constants for secondary sites in n-alkanes.[37,38]

Fate of cyclopentanone radicals

The 2-oxo-cyclopentyl radical is more stable than the 3-oxo isomer and the equilibrium constant approaches unity only at 1,850 K. Interconversion via a 1,3 hydrogen shift reaction is feasible with a barrier of 167 kJ mol^{-1} with an isomerization rate constant calculated to be $2.66 \times 10^{13}\exp(-20,393/T)$ s^{-1}. The half-life of a CPO-2 radical isomerizing to CPO-3 therefore is approximately 1 μs at 1,050 K. As will be evident below isomerization is slower than the competitive ring-opening reaction RO2 available to CPO-2. In a similar vein isomerization of 3-oxo to 2-oxo is *slower* than the corresponding fastest ring-opening reaction RO4.

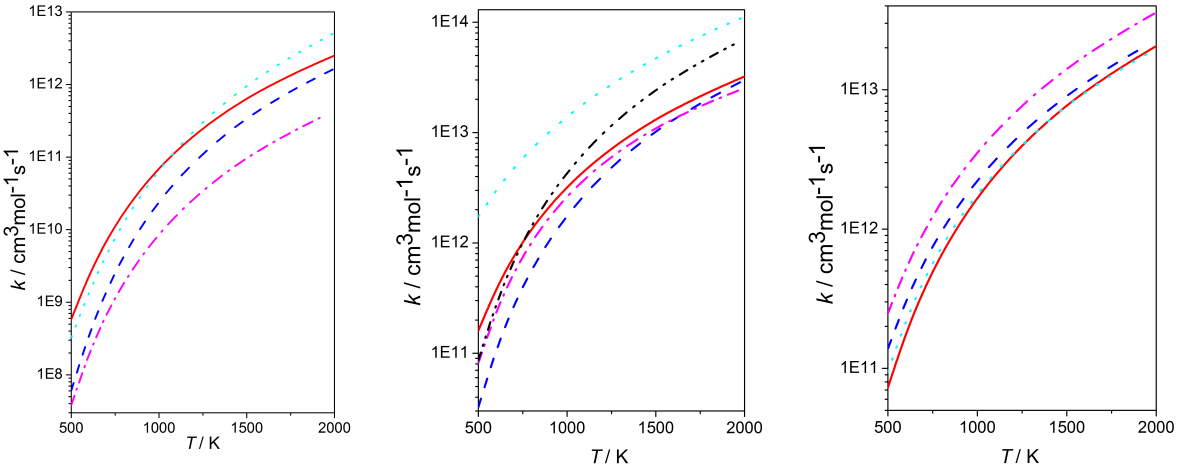

(a) (b) (c)

Figure 8: (a) H-abstraction by $\dot{C}H_3$ radicals from CPO to form CPO-2 (—), CPO-3 (– – –), from a β site in THF[34] (· · ·) and from $-CH_2-$ in an n-alkane[35] (– · –). (b) H-abstraction by $\dot{H}$ atom from CPO to form CPO-2 (—) and CPO-3 (– – –), from β site in THF[34] (· · ·), cyclopentane (– · –), from $-CH_2-$ in an n-alkane[36] (– · · –). (c) H-abstraction by $\ddot{O}$ atom from CPO to form CPO-2 (—), CPO-3 (– – –), from $-CH_2-$ in an n-alkane (· · ·),[37] (– · –)[38]

Table 2: H-abstraction by $\dot{H}$, $\ddot{O}$ and $\dot{C}H_3$; units kJ, mol, s; rate constants are for per H-atom

Site	$E^{\ddagger}$	$\Delta_r H$	A-factor	n	E_A
			$\dot{H}$ atom		
α eq	27.3	−60.9	2.64×10^{6}	2.185	18.1
α ax	20.0	−60.9	3.39×10^{6}	2.121	10.8
β eq	34.2	−33.8	2.05×10^{6}	2.259	24.6
β ax	28.1	−33.8	1.71×10^{6}	2.263	18.5
			$\ddot{O}$ atom		
α eq	21.6	−54.0	2.09×10^{5}	2.501	15.8
α ax	14.5	−54.0	1.33×10^{5}	2.389	8.6
β eq	18.2	−26.9	5.14×10^{4}	2.629	10.9
β ax	13.4	−26.9	7.03×10^{4}	2.522	6.6
			$\dot{C}H_3$ radical		
α eq	38.8	−57.6	5.49×10^{1}	3.270	25.2
α ax	32.1	−57.6	3.38×10^{1}	3.232	18.7
β eq	49.4	−30.5	8.48×10^{0}	3.483	33.2
β ax	44.7	−30.5	9.69×10^{0}	3.468	28.7

The initially formed CPO-2, and CPO-3 radicals can undergo β-scission reactions; thus, CPO-2 can ring-open via C3–C4 and C5–C1 scission, Fig. 9, whilst CPO-3 faces a similar choice between C4–C5 and C2–C1, Fig. 10. The computed barrier heights, in kJ mol^{-1}, for reactions RO1–RO4 are in reasonable agreement with those calculated by Scheer et al.[10]

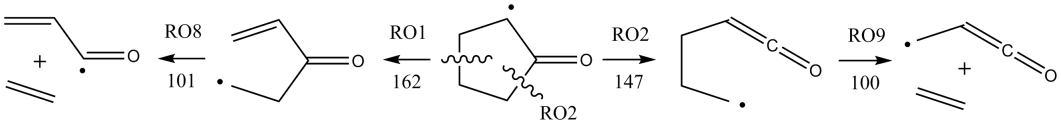

Figure 9: Reaction barriers of 2-oxo-cyclopentyl, kJ mol^{-1}.

Subsequent reactions of RO8, RO9 and RO5, RO7 produce species whose chemistry is somewhat better known; an additional channel RO6 is in competition with RO7 and leads to the same products as channel RO5, namely allyl radical + ketene but faces a larger barrier of 69 kJ mol^{-1}.

The calculated Arrhenius parameters for these reactions are listed in Table 3 from which it can be inferred that scission of the C1–C2 or C1–C5 bonds prevails over scission of the C3–C4 bond, that is k(RO2) > k(RO1) and k(RO4) > k(RO3) and the elimination of CO is much faster than the formation of allyl and ketene, k(RO7) >> k(RO6). Thus, the 3-oxo-cyclopentyl radical is more reactive and in the absence of other interfering reactions will primarily decompose by elimination of carbon monoxide to yield the 3-buten-1-yl radical, $H_2C{=}CH{-}CH_2{-}\dot{C}H_2$. Subsequent reactions of this radical, such as a 1,2-hydrogen shift to form an allylic system, $H_2C{\cdots}\dot{C}H{\cdots}CH_2CH_3$, have been thoroughly explored in recent times by Dean et al.[39] and Miyoshi.[40]

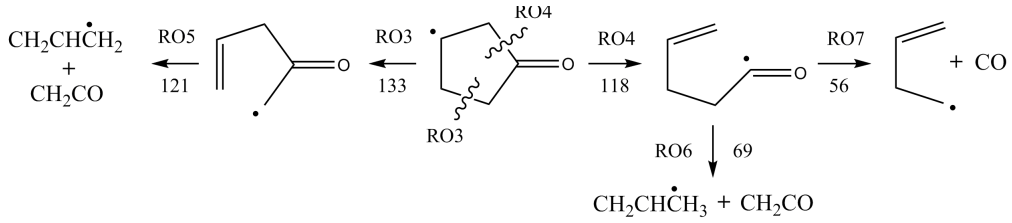

Figure 10: Reactions of 3-oxo-cyclopentyl / kJ mol^{-1}.

We note that species corresponding to $C_4H_7^+$ were detected by mass spectrometry in

the very recent flow tube experiments[10] of $Cl^{\bullet}$ + CPO at 550–650 K both in the presence *and* in the absence of O_2; which is a supporting evidence of the essential correctness of the ring-opening and β-scission routes calculated here.

Table 3: Arrhenius parameters for ring opening.

#	A-factor / s^{-1}	E_A / kJ mol^{-1}
RO1	1.32×10^{14}	169.5
RO2	9.50×10^{13}	153.5
RO3	1.39×10^{13}	138.1
RO4	1.72×10^{13}	121.8
RO5	3.92×10^{13}	127.1
RO6	5.50×10^{11}	68.7
RO7	6.08×10^{14}	65.1
RO8	1.68×10^{14}	105.7
RO9	5.69×10^{13}	104.6

In the Supplemental Material we have also compared the decomposition rate constants of RO1, RO2, RO3 and RO4 with similar reaction processes in the cyclopentane radical calculated by Wang[41] and Al Rashidi.[42]

Conclusions

The thermochemistry of cyclopentanone and its radicals has been computed. In addition, the C–H bond dissociation energies were also calculated to compare with existing literature values. Even though the comparisons do show some inconsistencies in the current literature, the discrepency between the calculation in this work and the ones in the literature is still within 4 kJ mol^{-1}.

We have carried out a systematic detailed study of the energetics and chemical kinetics of the hydrogen atom abstraction reactions from cyclopentanone by $\dot{H}$ and $\ddot{O}$ atoms and $\dot{O}H$, $H\dot{O}_2$ and $\dot{C}H_3$ radicals.

For H-atom abstraction by $\dot{O}H$ and $H\dot{O}_2$ radicals, pre- and post-complexes were formed in most of the reaction channels especially for abstractions at the α position.

The fate of the initially formed oxo-cyclopentyl radicals is delineated and it is shown that 3-oxo-cyclopentyl is more reactive than 2-oxo-cyclopentyl, and consequently, in accordance with very recent observations, production of 3-buten-1-yl radical and CO is favored.

The results of this work are suitable for inclusion in present-day detailed chemical kinetic mechanisms, replacing estimated values which have been determined by analogy. However, there are other reaction classes, for example, the reaction of CPO-2 radical with $H\dot{O}_2$ or of CPO-3 with molecular oxygen followed by subsequent isomerization and decomposition. These classes will be important in the low to intermediate temperature regimes, below 1000 K. Further ab initio calculations for those reaction classes will be needed to determine the rate constants for these reactions and allow accurate predictions by chemical kinetic models.

For hydrogen abstraction by species not considered by the present study, such as O_2 and other less important radicals, rate constants can be estimated by analogy to a secondary site in an *n*-alkene. In a similar vein other reactions will need to be estimated and/or computed in order to develop a comprehensive mechanism but the completion of this task and its validation against fundamental experimental data are beyond the scope of this work.

Acknowledgement

The work at NUI Galway was supported by Saudi Aramco under the FUELCOM program. The work at LLNL was conducted as part of the Co-Optimization of Fuels & Engines (Co-Optima) project sponsored by the U.S. Department of Energy (DOE) Office of Energy Efficiency and Renewable Energy (EERE), Bioenergy Technologies and Vehicle Technologies Offices and was performed under the auspices of the U.S. Department of Energy by Lawrence Livermore National Laboratory under Contract DE-AC52-07NA27344. Computational resources were provided by the Irish Centre for High-End Computing, ICHEC.

Supporting Information Available

Supplementary data associated with this article is available in the online version. It includes the geometries, vibrational frequencies, rotational constants and energies of each species mentioned in the article. This material is available free of charge via the Internet at `http://pubs.acs.org/`.

References

(1) Strobel, G. A.; Knighton, B.; Kluck, K.; Ren, Y.; Livinghouse, T.; Griffin, M.; Spakowicz, D.; Sears, J. The Production of Myco-diesel Hydrocarbons and their Derivatives by the Endophytic Fungus *Gliocladium roseum*. *Microbiol.* **2008**, *154*, 3319–3328.

(2) Griffin, M. A.; Spakowicz, D. J.; Gianoulis, T. A.; Strobel, S. A. Volatile Organic Compound Production by Organisms in the Genus *Ascocoryne* and a Re-evaluation of Myco-diesel Production by NRRL 50072. *Microbiol.* **2010**, *156* 3814–3829.

(3) Le Roux, E.; Chaouch, M.; Diouf, P. N.; Stevanovic, T. Impact of a Pressurized Hot Water Treatment on the Quality of Bio-oil Produced from Aspen. *Biomass Bioenergy* **2015**, *81*, 202–209.

(4) Yang, Y.; Dec, J. Bio-Ketones: Autoignition Characteristics and Their Potential as Fuels for HCCI Engines. Society of Automotive Engineers, SAE 2013-01-2627, **2013**.

(5) Harpster, M. Future Directions in Powertrain Light Duty Perspective. `https://www.erc.wisc.edu/symposium2015.php`, **2015**.

(6) Vaz, P. D.; Nolasco, M. M.; Ribeiro-Claro, P. J. A. Intermolecular CHO interactions in Cyclopentanone: An Inelastic Neutron Scattering Study. *Chem. Phys.* **2013**, *427*, 117–123.

(7) Zaras, A. M.; Dagaut, P.; Serinyel, Z. Computational Kinetic Study for the Unimolecular Decomposition Pathways of Cyclohexanone. *J. Phys. Chem. A* **2015**, *119*, 7138–7144.

(8) Serinyel, Z.; Togbé, C.; Zaras, A. M.; Dayma, G.; Dagaut, P. Kinetics of Oxidation of Cyclohexanone in a Jet-Stirred Reactor: Experimental and Modelling, *Proc. Combust. Inst.* **2015**, *35*, 507–514.

(9) Zaras, A. M.; Thion, S.; Dagaut, P. Computational Kinetic Study for the Unimolecular Decomposition of Cyclopentanone. *Int. J. Chem. Kinet.* **2015** *47* 439–446.

(10) Scheer, A. M.; Welz, O.; Vasu, S. S; Osborn, D. L.; Taatjes, C. A. Low Temperature (550–700 K) Oxidation Pathways of Cyclic Ketones: Dominance of HO_2-elimination Channels Yielding Conjugated Cyclic Coproducts. *Phys. Chem. Chem. Phys.* **2015** *17* 12124–12134.

(11) Xia, S.-H.; Liu, X.-Y.; Fang, Q.; Cui, G. Excited-State Ring-Opening Mechanism of Cyclic Ketones: A MS-CASPT2//CASSCF Study. *J. Phys. Chem. A.* **2015**, *119*, 3569–3576.

(12) Zhao, Y.; Truhlar, D. G. The M06 Suite of Density Functionals for Main Group Thermochemistry, Thermochemical Kinetics, Noncovalent Interactions, Excited States, and Transition Elements: Two New Functionals and Systematic Testing of Four M06-class Functionals and 12 other Functionals. *Theor. Chem. Acc.* **2008**, *120* 215–241.

(13) Fukui, K. The Path of Chemical Reactions — the IRC Approach. *Accounts Chem. Res.* **1981**, *14* 363–368.

(14) Hratchian, H. P.; Schlegel, H. B. in: C. E. Dykstra, G. Frenking, K. S. Kim, G. E. Scuseria, (Eds.) Finding Minima, Theory and Applications of Computational Chemistry: The First 40 Years, Elsevier, Amsterdam, **2005** pp. 195–249.

(15) Woon,,D. E. Jr; Dunning, T. H. Gaussian Basis Sets for use in Correlated Molecular Calculations. V. Core-valence Basis Sets for Boron through Neon. *J. Chem. Phys.* **1995**, *103*, 4572–4585.

(16) Halkier, A.; Helgaker, T.; Jorgensen, P.; Klopper, W.; Koch, H.; Olsen, J.; Wilson, A. K. Basis-Set Convergence in Correlated Calculations on Ne, N_2, and H_2O. *Chem. Phys. Lett.* **1998**, *286*, 243–252.

(17) Lee, T. J.; Rendell, A. P.; Taylor, P. R. Comparison of the Quadratic Configuration Interaction and Coupled-cluster Approaches to Electron Correlation including the Effect of Triple Excitations. *J. Phys. Chem.* **1990**, *94*, 5463–5468.

(18) Werner, H.-J.; Knowles, P. J.; Knizia, G.; Manby, F. R.; Schütz, M. *WIREs Comput Mol Sci.* **2012**, *2*, 242-253. MOLPRO, version 2010.1, a package of ab initio programs, Werner, H.-J.; Knowles, P. J.; Knizia, G.; Manby, F. R.; Schütz, M.; Celani, P.; Korona, T.; Lindh, R.; Mitrushenkov, A.; Rauhut, G., et al. `http://www.molpro.net`.

(19) Curtiss, L. A.; Redfern, P. C.; Raghavachari, K., Gaussian-4 Theory. *J. Chem. Phys.* **2007**, *126*, 084108.

(20) Gaussian 09, Revision E.01, Frisch, M. J.; Trucks, G. W.; Schlegel, H. B.; Scuseria, G. E.; Robb, M. A.; Cheeseman, J. R.; Scalmani, G.; Barone, V.; Mennucci, B.; Petersson, G. A.; et al. Gaussian, Inc., Wallingford CT, 2009.

(21) Eckart, C. The Penetration of a Potential Barrier by Electrons. *Phys. Rev.* **1930**, *35* 1303–1309.

(22) Klippenstein, S. J.; Wagner, A. F.; Dunbar, R. C.; Wardlaw, D. M.; Robertson, S. H.; Miller, J. A. Variflex 2.02m, 2010.

(23) MultiWell-2013 Software, Jan 2013, designed and maintained by J.R. Barker with contributors N.F. Ortiz, J.M. Preses, L.L. Lohr, A. Maranzana, P.J. Stimac, T. L. Nguyen, and T. J. Dhilip Kumar, University of Michigan, Ann Arbor, MI; `http://aoss.engin.umich.edu/multiwell/`.

(24) Barker, J. R. Multiple-Well, Multiple-Path Unimolecular Reaction Systems. I. MultiWell Computer Program Suite. *Int. J. Chem. Kinetics* **2001**, *33*, 232–245 .

(25) Luo, Y.-R. Comprehensive Handbook of Chemical Bond Energies. CRC Press: Boca Raton, FL, **2007**.

(26) Simmie, J. M.; Somers, K. P., Benchmarking Compound Methods (CBS-QB3, CBS-APNO, G3, G4, W1BD) against the Active Thermochemical Tables: A Litmus Test for Cost-Effective Molecular Formation Enthalpies. *J. Phys. Chem. A* **2015**, *119*, 7235–7246.

(27) Wiberg, K.B.; Crocker, L.S.; Morgan, K.M. Thermochemical studies of carbonyl compounds. 5. Enthalpies of reduction of carbonyl groups. *J. Am. Chem. Soc.* **1991**, *113*, 3447–3450.

(28) Wolf, G. Thermochemische Untersuchungen an cyclischen Ketonen. *Helv. Chim. Acta 1972*, *55* 1446–1459.

(29) Sellers, P.; Sunner, S. Heats of Combustion of Cyclic Ketones and Alcohols. *Acta Chem. Scand.* **1962**, *16* 46–52.

(30) Zwolinski, B. J.; Beach, L. Selected Values of Properties of Chemical Compounds., Thermodynamics Research Center, Texas A&M University, College Station, Texas, 1997.

(31) Georgievskii, Y.; Klippenstein, S. J. Strange Kinetics of the C_2H_6 + CN Reaction Explained. *J. Phys. Chem. A. 2007*, *111*, 3802–3811.

(32) Galano, A.; Alvarez-Idaboy, J. R. in: E. G. Michael, S. J. Matthew, (Eds.) Advances in Quantum Chemistry, Academic Press: **2008**; *55*, pp 245–274.

(33) Dagaut, P.; Wallington, T. J.; Liu, R. Z.; Kurylo, M. J. A Kinetic Investigation of the Gas-phase Reactions of Hydroxyl Radicals with Cyclic Ketones and Diones: Mechanistic Insights. *J. Phys. Chem. A* **1988**,*92*, 4375–4377.

(34) Simmie, J. M. Kinetics and Thermochemistry of 2,5-Dimethyltetrahydrofuran and Related Oxolanes: Next Next-Generation Biofuels. *J. Phys. Chem. A 116* (2012) 4528–4538.

(35) Manion, J. A.; Sheen, D. A.; Awan, I. A. Evaluated Kinetics of the Reactions of H and CH3 with n-Alkanes: Experiments with n-Butane and a Combustion Model Reaction Network Analysis. *J. Phys. Chem. A* **2015**, *119* 7637–7658.

(36) Sarathy, S. M.; Javed, T.; Karsenty, F.; Heufer, A.; Wang, W.; Park, S.; Elwardany, A.; Farooq, A.; Westbrook, C. K.; Pitz, W. J.; Oehlschlaeger, M. A.; Dayma, G.; Curran, H. J.; Dagaut, P. A Comprehensive Combustion Chemistry Study of 2,5-Dimethylhexane. *Combust. Flame* **2014**, *161*, 1444–1459.

(37) Tsang, W. Chemical Kinetic Data Base for Combustion Chemistry. Part 3: Propane. *J. Phys. Chem. Ref. Data* **1988**, *17*, 887–951.

(38) Cohen, N.; Westberg, K. R. Chemical Kinetic Data Sheets for HighTemperature Reactions. Part II. *J. Phys. Chem. Ref. Data* **1991**, *20*, 1211–1267.

(39) Wang, K.; Villano, S. M.; Dean, A. M. The Impact of Resonance Stabilization on the Intramolecular Hydrogen-Atom Shift Reactions of Hydrocarbon Radicals. *ChemPhysChem* **2015**, *16*, 2635–2645.

(40) Miyoshi, A. Computational Studies on the Reactions of 3-Butenyl and 3-Butenylperoxy Radicals. *Int. J. Chem. Kinet.* **2010**, *42*, 273–288.

(41) Wang, K.; Villano, S. M.; Dean, A. M. Reactivity-Structure-Based Rate Estimation Rules for Alkyl Radical H Atom Shift and Alkenyl Radical Cycloaddition Reactions. *J. Phys. Chem. A* **2015** *119* 7205–7221.

(42) Al Rashidi, M. J.; Thion, S.; Togbé, C.; Dayma, G.; Mehl, M.; Dagaut, P.; Pitz, W. J.; Zádor, J.; Sarathy, S. M. Elucidating Reactivity Regimes in Cyclopentane Oxidation: Jet Stirred Reactor Experiments, Computational Chemistry, and Kinetic Modeling. *Proc. Combust. Inst.* (doi:http://dx.doi.org/10.1016/j.proci.2016.05.036).

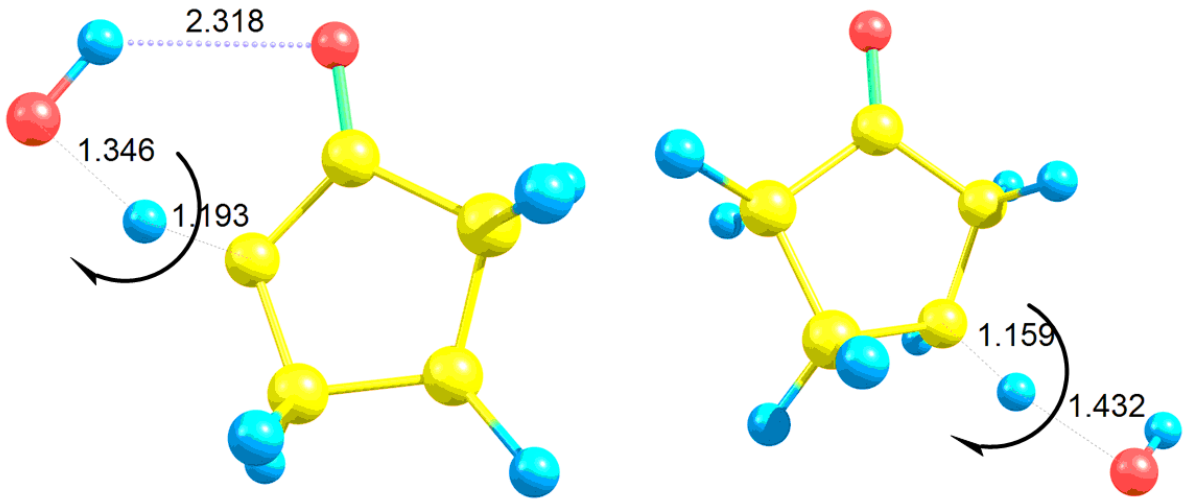

Fig: TOC graphic